

Journal of Materials Chemistry A

Accepted Manuscript



This is an *Accepted Manuscript*, which has been through the Royal Society of Chemistry peer review process and has been accepted for publication.

Accepted Manuscripts are published online shortly after acceptance, before technical editing, formatting and proof reading. Using this free service, authors can make their results available to the community, in citable form, before we publish the edited article. We will replace this *Accepted Manuscript* with the edited and formatted *Advance Article* as soon as it is available.

You can find more information about *Accepted Manuscripts* in the [Information for Authors](#).

Please note that technical editing may introduce minor changes to the text and/or graphics, which may alter content. The journal's standard [Terms & Conditions](#) and the [Ethical guidelines](#) still apply. In no event shall the Royal Society of Chemistry be held responsible for any errors or omissions in this *Accepted Manuscript* or any consequences arising from the use of any information it contains.

Cite this: DOI: 10.1039/c0xx00000x

www.rsc.org/xxxxxx

ARTICLE TYPE

Light-healable hard hydrogels through photothermally induced melting-crystallization phase transition

Hongji Zhang,^a Dehui Han,^a Qiang Yan,^a Daniel Fortin,^a Hesheng Xia^{*b} and Yue Zhao^{*a}

Received (in XXX, XXX) Xth XXXXXXXXXX 20XX, Accepted Xth XXXXXXXXXX 20XX

DOI: 10.1039/b000000x

A general method for preparing mechanically strong hydrogels that can undergo light-triggered healing was demonstrated. By loading a small amount of gold nanoparticles (AuNPs, 0.05 wt%) in hydrogel prepared with stearyl acrylate (SA), N,N-dimethylacrylamide (DMA) and N,N'-methylenebisacrylamide (MBA), whose strength is endowed by chemical crosslinking coexisted with crystallized hydrophobic SA side chains acting as the physical crosslinks, exposing a cut-through damage to laser of wavelength at the surface plasmon resonance of AuNPs and subsequently turning off the light, gives rise to efficient healing of the hydrogel as a result of the reversible melting-crystallization phase transition of the hydrophobically associated SA chains. Hydrogel of this kind exhibits unprecedented tensile strength after repairing greater than 2 MPa. It also displays light-controllable shape memory effect.

15

Introduction

Hydrogels, made from natural or synthetic polymers, hold an important place in smart and soft materials due to their applications in many areas such as biomedicine,¹ biosensors,² soft robotics³ and tissue scaffolds.⁴ In particular, inspired by nature, polymer hydrogels capable of self-repairing damage have attracted much attention in recent years. Up to date, a variety of strategies have been successfully developed to enable hydrogels self-healing, including the use of hydrogen bonding,⁵ electrostatic interactions,⁶ dynamic chemical bonds,⁷ π - π stacking,⁸ ion migration,⁹ molecular recognition,¹⁰ metal coordination,¹¹ molecular diffusion¹² and hydrophobic associations with surfactant.¹³ However, self-healable hydrogels as well as hydrogels healable under the effect of a stimulus (generally heating) are soft materials of low mechanical strength. This weakness prevents them from some stress-bearing applications such as cartilage and tissue engineering scaffolds. To our knowledge, the magnitude of the tensile strength regained after repairing for most healable hydrogels is below 0.4 MPa. Only few mechanically strong healable hydrogels were reported recently. For example, Gong et al^{6d} demonstrated polyampholyte hydrogels (water content 50-70 wt%, original strength as high as 2 MPa) which showed partial self-healing in salt solution or at an elevated temperature in water (50 °C) with a recovered strength of around 0.38 MPa. Wang et al^{5d} reported graphene-reinforced nanocomposite hydrogel (water content ~78 wt%) exhibiting high tensile strength up to 0.35 MPa after repairing at an elevated temperature. The challenge of making self- or stimuli-healable strong hydrogels is inherent. Efficient healing of a hydrogel requires high polymer chain mobility and diffusion in the damaged region, which normally means low mechanical strength.

This is the reason for which healable hydrogels are usually made with dynamic networks or physically crosslinked systems, while self-healing of permanently crosslinked hydrogels with high crosslinking density for mechanical strength, has remained largely inaccessible because of the much reduced chain mobility. Herein we demonstrate a general method for preparing light-healable strong hydrogel. We show that the tensile strength after optical healing of cut-through damage can reach > 2 MPa for hydrogel prepared by copolymerization of stearyl acrylate (SA), N,N-dimethylacrylamide (DMA) and N,N'-methylenebisacrylamide (MBA), containing 0.05 wt% of gold nanoparticles (AuNPs) surface-functionalized with poly(N-acryloyl 6-aminocaproic acid) (PA6ACA).

60

Experimental

The key steps for preparing the strong hydrogel containing AuNPs are described below. Additional details on the synthesis and characterizations are given in Supporting Information.

Synthesis of PA6ACA-functionalized AuNPs: To a vigorously stirred solution containing HAuCl₄·3H₂O (39.4 mg, 0.1 mmol) and PA6ACA (0.8 g, 0.2 mmol) in 40 mL MeOH, NaBH₄ (0.3 mmol) in 3 mL MeOH was added dropwise under cooling in an ice bath. The solution rapidly turned red and it was kept under stirring for another 3 h at room temperature. Afterwards, three consecutive centrifugations at 28,000 rpm were carried out to collect AuNPs and remove free polymer chains. The obtained AuNPs can readily be dispersed in MeOH, DMSO or water.

Synthesis of AuNP-containing Hydrogels: The AuNP-loaded, chemically cross-linked P(DMA-SA) hydrogel was prepared by using an in-situ free radical copolymerization method. As an

example, AIBN (7 mg, 0.043 mmol, initiator), MBA (3.8 mg, 0.025 mmol, covalent crosslinker), SA (105 mg, 0.324 mmol), DMA (125 mg, 1.263 mmol), AuNP (0.115 mg in 0.1 mL MeOH) and 0.5 mL ethanol were introduced into a flat-bottom vial with a sealable cap. The mixture was first pre-heated to 40 °C to obtain a homogeneous solution and then immersed into an oil bath at 85 °C for 30 min to afford the in-situ free radical copolymerization. Afterwards, the as-synthesized cross-linked gel was completely dried under vacuum at room temperature before being soaked in a large amount of water for at least two weeks to remove un-crosslinked water-soluble species and for the hydrogel to reach its equilibrium swelling state. In addition, following the same procedure and under the same conditions, replacing SA with lauryl acrylate (LA), hexyl acrylate (HA) or ethyl acrylate (EA) allowed us to prepare AuNP-containing hydrogels in which the hydrophobic side chains are shorter than SA.

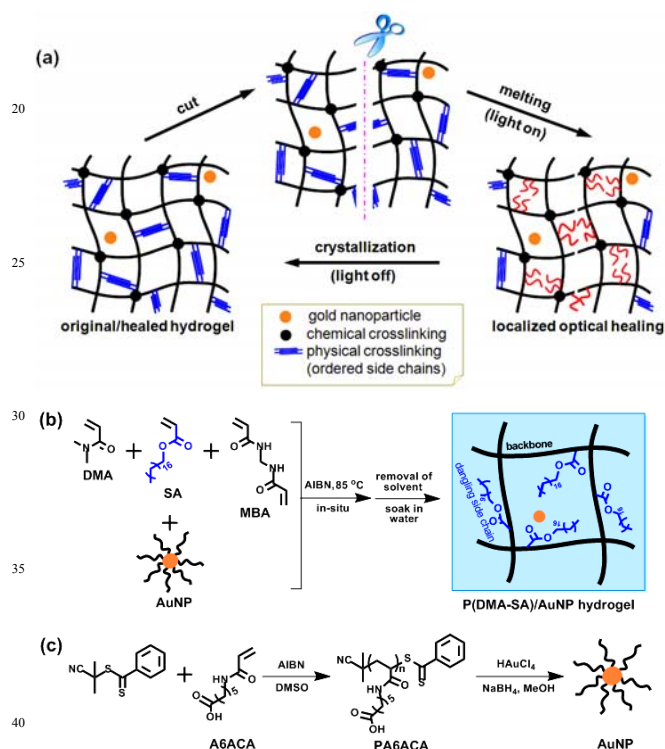


Figure 1. (a) Schematic illustration of light-healable strong hydrogel based on a photothermally induced melting-crystallization phase transition of the physical crosslinks; (b) synthesis of crosslinked P(DMA-SA)/AuNP hybrid hydrogel with hydrophobic side chains for physical crosslinking through crystallization; and (c) synthesis of PA6ACA-capped AuNPs.

Results and Discussion

Figure 1a schematically depicts the used method. A small amount of AuNPs is added in a mechanically strong hydrogel prepared using a strategy first reported by Osada et al. for imparting the shape-memory effect.^{14a, f} The hydrogel is built up with chemical crosslinking coexisting with crystallized hydrophobic long alkyl side chains acting as physical crosslinks; the physical network allows for fixation of a temporary shape and its dissociation enables the recovery of the permanent shape.¹⁴ On the other hand, hydrogel capable of self-healing at room temperature through

hydrophobic associations of alkyl side chains was first demonstrated by Tuncaboylu et al.¹³ by making use of the dynamic nature of physical crosslinks stabilized by micelles of a surfactant. In our case, to achieve optical healing of strong hydrogel, a laser of wavelength close to the surface plasmon resonance (SPR) of AuNPs is applied to the fracture surfaces of the hydrogel (e.g. cut); heat released by AuNPs due to SPR can raise the temperature locally in the exposed damage area and induce the melting of the physical crosslinks so that the melt chains can inter-diffuse in the fractured region. When laser is turned off, the crystallization of the hydrophobic side chains takes place on cooling that binds the fracture surfaces for healing. In principle, without AuNPs in the hydrogel, direct heating should also work for healing. However, the advantage of using the AuNP SPR-based photothermal effect is the ability to confine the heating only in spatially selected area, i.e. only on damage without affecting the rest of the hydrogel, as well as the capacity of remote activation of the healing process. Thermal effect induced by external stimuli such as light, ultrasound and magnetic field have been exploited for polymer self-healing and shape memory¹⁵, but we are unaware of any report of this kind. Figure 1b shows the formulation of our hydrogel that basically is a random copolymer of DMA (as water-soluble polymer), SA (for long alkyl side chains) and MBA (for covalent crosslinking). While the hydrophilic DMA is for water uptake, the hydrophobic SA provides dangling side chains that aggregate and crystallize to constitute the physical crosslinks of the hydrogel. The P(DMA-SA)/AuNP hybrid hydrogel was prepared by in-situ free radical copolymerization of the mixture of the monomers in the presence of AuNPs (Figure 1b). To ensure good dispersion of AuNPs in the hydrogel, as shown in Figure 1c, the nanoparticles were synthesized by using a reduction method in the presence of dithiobenzoate-terminated PA6ACA ligand. Upon addition of the reducing agent NaBH₄, the dithiobenzoate end group was converted to the thiol group attached onto the surface of AuNPs, resulting in AuNPs (2.5-10 nm in diameter) surface-functionalized with PA6ACA that is a polyacrylamide favoring the compatibility of AuNPs with the hydrogel.

Table 1. Prepared hydrogel samples with varying SA and MBA contents for physical and covalent crosslinking, respectively, as well as their water content and thermal properties indicating the reversible melting-crystallization phase transition of the hydrophobic SA side chains in most samples (T_m : melting temperature on heating; T_c : crystallization temperature on cooling; ΔH : melting enthalpy; X_c : crystallinity).

Sample	MBA ^[a] (mol%)	SA ^[a] (mol%)	Water content (wt%)	T_m (°C)	T_c (°C)	ΔH ^[b] (J/g)	X_c ^[c] (%)
1	1.5	24	50	45.4	38.3	25.2	44.3
2	1.5	20	56	42.9	36.1	6.6	15.3
3	1.5	16	61	39.8	32.5	0.7	2.1
4	1.5	10	70	–	–	–	–
5	2.7	24	47	44.2	37.4	23.1	38.3
6	6.0	24	42	41.1	35.3	13.8	20.9
7	15.0	24	38	–	–	–	–

[a] with respect to the total amount of monomers; [b] calculated with respect to the weight of hydrogel; [c] calculated by using $\Delta H^0=218$ J/g for 100% crystallized SA side chains.¹⁶

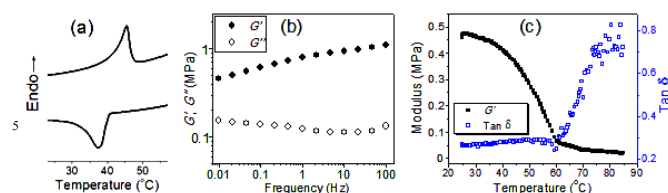


Figure 2. Characterization of the hydrogel containing 1.5% MBA and 24% SA: (a) DSC heating and cooling curves; (b) changes in the storage modulus, G' and loss modulus, G'' , of the hydrogel as a function of frequency at room temperature; and (c) changes in the storage modulus and $\tan\delta$ as a function of temperature at a fixed frequency of 1 Hz. All heating or cooling experiments were carried out at a rate of 5 °C/min.

Table 1 lists the hydrogel samples prepared by varying the density of either the covalent or the physical crosslinks. At a given concentration of MBA, the amount of SA determines the extent of hydrophobic associations and crystallization of the SA side chains (samples 1-4). Whereas at a constant SA content, changing the concentration of MBA results in hydrogels of different covalent crosslinking density (samples 1 and 5-7). The effects of these parameters on the optical healing will be discussed later. In all samples, the amount of AuNPs was kept at 0.05 wt% with respect to the total amount of monomers. Unless otherwise stated, the results obtained with sample 1, i.e., the hydrogel prepared with 1.5% crosslinker MBA and 24% SA with hydrophobic side chains, will be presented and used for discussion. Figure 2 shows the characterization results for this hydrogel. At room temperature, the swelling degree at equilibrium (weight ratio of gel containing water over dried gel) is ~ 2 , meaning that the hydrogel contains ~ 50 wt% of water. This level of water content is relatively low with respect to some tough hydrogels.^{6c, d} The DSC curves in Figure 2a display an endothermic peak at 45 °C on heating and an exothermic peak at 38 °C on cooling, resulting from the melting and crystallization, respectively, of the alkyl side chains in the hydrogel. Figure 2b shows the storage and loss modulus of the sample as a function of frequency at room temperature. Over the whole frequency range, the hydrogel behaves like a solid with much higher storage modulus. Figure 2c shows the change in the storage modulus and in $\tan\delta$ (ratio of G'' to G') vs. temperature at a fixed frequency of 1 Hz. The hydrogel starts to lose the stiffness at temperature above 42 °C, dropping from around 0.4MPa at this temperature to 0.04 MPa at 60 °C. Such drastic change in the mechanical property should be attributed to the thermally induced phase transition from ordered (crystalline) packing to disordered (amorphous) aggregate of the SA side chains. The concomitant increase of $\tan\delta$ also confirms the softening of the hydrogel associated with the disruption of the physical crosslinks.

Efficient optical healing of the strong hydrogel is depicted in Figure 3. One original sample was cut into two (Figure 3a-b); the two halves were brought into intimate contact and then a diode laser beam ($\lambda = 532$ nm, 0.72 W, beam diameter ~ 3 mm) was applied to the interfacial area for 5 seconds (scanning along the junction of the two surfaces) and the two halves merged into one single piece after turning off the laser (Figure 3c). Here it should be noted that without laser exposure no healing effect could be observed no matter how long the two halves were held in contact. Likewise, without AuNPs in the hydrogel, no healing was

possible under the used conditions. To further evaluate quantitatively the optical healing efficiency, tensile tests were performed on the original and the optically healed hydrogel samples with short laser irradiation times. After turning off the laser and before conducting the mechanical tests, the healed hydrogel samples were rest at room temperature for a few minutes for thermal equilibrium. The results of tensile test are shown in Figure 3d.

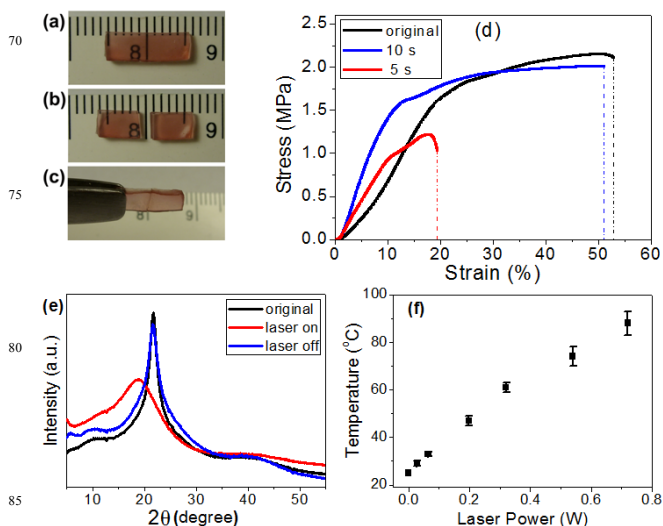


Figure 3. Optical healing of the hydrogel containing 1.5% MBA and 24% SA, enabled by the melting-crystallization phase transition of the hydrophobic side chains: (a-c) photos that visually show the healing behavior: (a) an original hydrogel sample, (b) the sample cut into two pieces and (c) healed sample emerging into one piece upon exposure to laser ($\lambda = 532$ nm, 0.72 W) for 5 seconds (c); (d) stress-strain curves for the original and optically healed hydrogels with two short laser (0.72 W) exposure times at room temperature; (e) x-ray diffraction patterns of the hydrogel sample recorded at room temperature, before exposure to laser, upon laser exposure (0.32 W) and after turning off the laser; and (f) the local temperature rise in the hydrogel as a function of applied laser power.

Upon elongation, the original hydrogel sample fractured at a stress of ~ 2.3 MPa and a strain of $\sim 50\%$. For the optically healed sample, whose fracture upon elongation occurred in the initial cut, a significant healing effect was achieved using just 5 seconds of light exposure at an intensity of 0.72 W, with the regained tensile strength reaching > 1 MPa. For the same hydrogel, after prolonging the laser exposure to 10 seconds, upon elongation the breaking of the healed sample took place at a higher tensile strength, which is also the strength at fracture in this case, close to 2 MPa, indicating an almost complete recovery of its original mechanical properties. It should be emphasized that to date, very few healable hydrogels were reported to exhibit a tensile strength recovered after repairing greater than 1 MPa. Experimental evidence supported the working hypothesis that a photo-thermally induced melting-crystallization phase transition inside the physical crosslinks is at the origin of the healing process. Figure 3e shows the X-ray diffraction pattern of a hydrogel sample where the sharp diffraction peak at $2\theta \sim 21.7^\circ$ arises from crystallized SA side chains. Upon laser exposure, only a broadened halo was observable around $2\theta \sim 19.1^\circ$

indicating disappearance of the ordered phase. Subsequently, after turning off the laser, the diffraction peak characteristic of a crystalline phase reappeared. This result confirmed that under the used conditions laser exposure could melt the crystalline domains packed by the dangling SA chains in the hydrogel, which was followed by a recrystallization occurring on cooling after turning of the laser. Moreover, by embedding a digital thermocouple into the hydrogel, it was possible to measure the local temperature rise in the close vicinity of the laser-exposed region. Figure 3f shows the detected temperature as a function of the applied laser power. With the used 0.72 W, the temperature detected rose quickly, < 4 seconds, above the melting temperature of about 45 °C. Back to Fig.3d, the Young's moduli at small strain for the optically healed samples appear to be higher than that of the original sample, which may be caused by a different state of crystallized SA chains and probably some drying effect in the cut region exposed to laser. However, this drying effect, if there is any, should be minimal due to the short laser exposure time; visually no change of the hydrogel could be noticed.

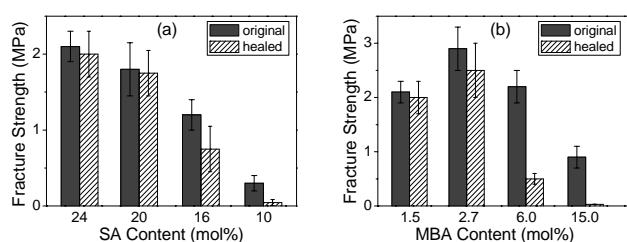


Figure 4. Comparison of the strength at fracture between the original and optically healed sample (10 seconds laser exposure, 0.72 W) for hydrogels of various compositions: (a) hydrogels with 1.5% of covalent crosslinker MBA but different SA contents (samples 1-4 in Table 1); and (b) hydrogels with 24% of SA but different covalent crosslinker contents (samples 1 and 5-7 in Table 1). Error bars represent the standard deviation ($n \geq 4$).

The results summarized in Figure 4 not only illustrate the effect of both the covalent and physical crosslinks on the healing, but also further confirm the optical healing mechanism and points out how to make the healing effective for mechanically strong hydrogels. Figure 4a compares the strength at fracture of undamaged hydrogel and the recovered fracture strength after optical healing (10 seconds laser exposure on two cut pieces, 0.72 W) for hydrogel samples with various contents of SA while having the same covalent crosslinker concentration (1.5%). As the SA content decreases, the initial fracture strength of the hydrogel decreases, which is understandable because less SA side chains means reduced contribution of the physical crosslinks to the mechanical strength. However, down to 20% SA, there is still an appreciable amount of crystallized SA chains for physical crosslinking in the hydrogel (Table 1), and the optical healing efficiency remains very high. The healing capability of the hydrogel starts to drop with 16% SA, for which only a very slight melting and crystallization of SA can be observed (Figure S4a). At 10% SA, it is no surprise to see basically the absence of healing because of the absence of crystallization of SA side chains. On the other hand, Figure 4b reports the data for hydrogels having the same physical crosslinking density with 24% SA but varying covalent crosslinking density with different

MBA contents. When the covalent crosslinker concentration increases from 1.5 to 2.7%, the hydrogel becomes even stronger exhibiting a fracture tensile strength approaching 3 MPa. At this level of covalent crosslinking, the dangling SA side chains can still associate and crystallize (Table 1); consequently, the optical healing efficiency remains excellent since the hydrogel showed recovered fracture strength near 2.5 MPa. By contrast, with the MBA concentration further up to 6%, the healing efficiency drops considerably even though an appreciable amount of crystallized SA chains exists in the hydrogel. This result implies that when the polymer chain mobility is restricted too much by the covalent crosslinking, the SA side chains melted under laser exposure can no longer sufficiently inter-diffuse in the damage region that is required for healing of the hydrogel after the laser is turned off. At the highest concentration of 15% covalent crosslinks, no melting-crystallization phase transition of SA chains could be detected (Figure. S4b) and, concomitantly, no optical healing was achievable. It is worth noting that in this last hydrogel, despite the very high covalent crosslinking density, its fracture strength is much smaller than the other hydrogels due to the absence of physical networking. This result indicates that high mechanical strength of this type of hydrogels comes from an appropriate balance of the covalent and physical crosslinking densities.

The crucial role played by crystallization of the SA side chains in the optical healing was also revealed by an additional control experiment. Various hydrogels containing hydrophobic alkyl side chains shorter than SA were synthesized under otherwise the same conditions. Figure 5 shows the used acrylate monomers and the results of the comparative optical healing measurements using samples prepared with the same MBA concentration (1.5%) and the same fraction of hydrophobic side chains (24%). No crystallization of all the shorter alkyl side chains was observed in the corresponding hydrogels. Consequently, not only the optical healing cannot develop in those hydrogels, but also their mechanical strength is weak as compared to the hydrogel with the SA side chains. We also mention that the efficiency of repeated optical healing of the same cut was investigated using the sample with 24% SA and 1.5% MBA. The recovered strength at fracture decreased slightly with increasing the number of fracture-healing cycles. The average tensile strength over five cycles was about 1.5 MPa.

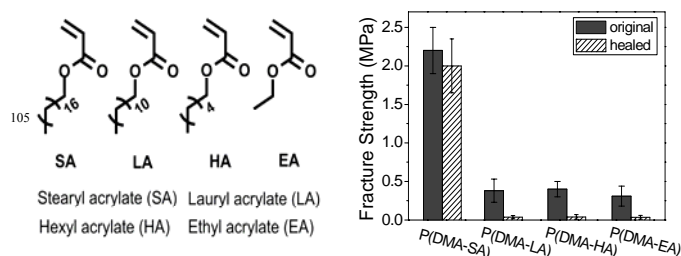


Figure 5. Chemical structures of the acrylates used in preparing the hydrogels with hydrophobic side chains of different lengths; and (b) comparison of the strength at fracture for the original and optically healed hydrogels (10 seconds laser exposure, 0.72 W). Except the nature of the acrylate comonomer, all hydrogels were prepared under the same conditions of 0.05 wt% AuNP, 1.5% MBA crosslinker and 24% of the comonomer. Error bars represent the standard deviation ($n \geq 4$).

At this point, we wish to emphasize that the main appealing feature of our AuNP-containing hydrogel is the ability of recovering a high tensile or fracture strength (not toughness) through optical healing. The loading of the very small amount of 0.05% of AuNPs is to ensure light-induced local heating for the melting of crystallized SA side chains, but not for enhancing the mechanical properties of the hydrogel, which differs from the self-healable nanocomposite hydrogels reported by Aida group^{6b} and others^{5c} containing a much larger amount of clay. Also, despite the fact that the other hydrogels prepared with shorter alkyl side chains (Fig.5) showed no optical healing effect, the demonstrated method is general in the sense that based on the melting-crystallization mechanism, any hydrogel with chemical and/or physical crosslinking could exhibit the optical healing capability if the physical crosslinks are provided by crystalline domains.

Moreover, it is worth being reported that our AuNP-containing hydrogel is multifunctional exhibiting optically controllable shape memory effect as well. As mentioned above, such coexisted physical crosslinks formed by a microphase separated component including the dangling hydrophobic side chains,^[14a] makes it possible to fix a temporary shape and their dissociation or softening activates the permanent shape recovery. Figure 6 shows an example of results. A piece of the hydrogel prepared with 1.5% MBA and 20% SA (sample 2 in Table 1) containing about 56 wt% of water was stretched to ~100% strain at 70 °C in a water bath followed by cooling to room temperature to afford fixation of the elongated temporary shape (photos a and b). When laser (0.32 W) was applied to the two end areas (about 2/3 of the length) at room temperature, a selective shape recovery was achieved in a few seconds with the sample contracting from both sides, while the unexposed middle part of the hydrogel remained intact (photo c). Subsequently, another exposure was exerted on the middle section to fulfill the whole shape recovery (photo d). Such optically controllable shape-memory effect originates from chain relaxation (or strain energy release) due to local temperature rise above the melting of the crystallized SA side chains (dissociation of the physical network). This can readily be confirmed by monitoring the force required to hold a hydrogel sample at a constant length upon laser exposure. Figure 6e shows the results for a hydrogel deformed to 50% strain (temporary shape) and, for comparison, the hydrogel of initial shape. Upon laser exposure, the unstretched sample displays a decrease of the stress, which is caused by thermal softening and expansion of the sample related to the melting of the SA side chains. By contrast, when laser was applied to the sample of temporary shape, despite the thermal expansion effect, a net increase in the stress was observed due to the restoring (contraction) force arising from the shape recovery process. Finally, we note that it is possible to optically heal a localized damage on a sample with a temporary shape without affecting the shape memory function, provided that the laser beam is focused on the damaged area so that other parts of the sample avoid photoinduced heating.

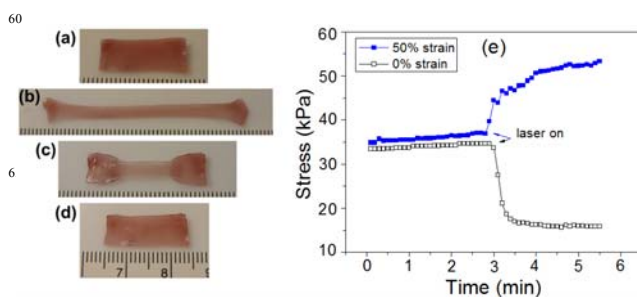


Figure 6. Light-controlled shape-memory behaviour of the hydrogel: photos of (a) a hydrogel of original shape, (b) the temporary shape obtained by stretching the sample to ~100% strain at 70 °C in a water bath followed by cooling to room temperature, (c) selective shape recovery by exposing the two end areas (about 2/3 of the sample) to laser (0.32 W), and (d) fully recovered permanent shape after laser exposure of the central part of the sample; (e) different changes in the stress required to hold a hydrogel sample with either original shape or temporary shape (deformed to 50% strain) upon exposure to laser (0.32 W).

Conclusion

In conclusion, we reported the use of photothermal effect induced melting-crystallization phase transition of hydrophobic alkyl side chains to prepare light-healable, mechanically strong hydrogels with high tensile strength after healing. The demonstrated mechanism makes the method general and applicable to preparing other strong stimuli-healable hydrogels. The key requirement in using this method is to have hydrophobically associated and crystallized side chains that constitute the physical crosslinks coexisting with permanent crosslinking for ensuring the mechanical strength of the hydrogels. The AuNP-containing hydrogel also exhibits light-controllable shape memory effect based on the melting-crystallization mechanism.

YZ acknowledges the financial support from the Natural Sciences and Engineering Research Council of Canada (NSERC) and le Fonds de recherche du Québec: Nature et technologies (FRQNT). HZ thanks China Scholarship Council (CSC) for a scholarship allowing him to study in Canada. HX. acknowledges financial support from major project of Chinese Ministry of Education (313036), the Programme of Introducing Talents of Discipline to Universities (B13040), and National Natural Science Foundation of China (51203102, 51010004); YZ is a member of the FRQNT-funded Center for Self-Assembled Chemical Structures (CSACS) and Centre québécois sur les matériaux fonctionnels (CQMF).

Notes and references

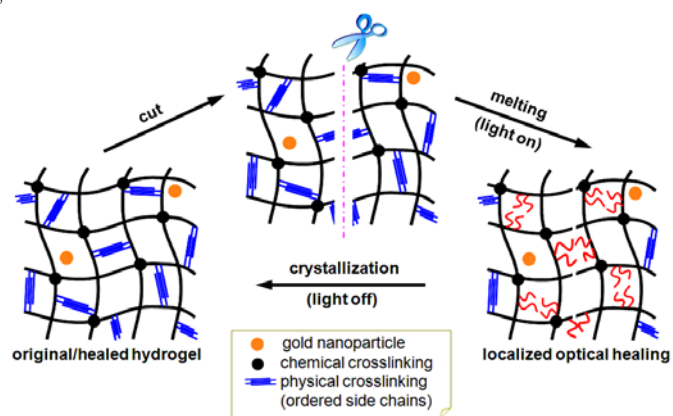
- ¹⁰⁵ ^a Département de chimie, Université de Sherbrooke, Sherbrooke, Québec, J1K 2R1, Canada. yue.zhao@usherbrooke.ca
^b State Key Laboratory of Polymer Materials Engineering, Polymer Research Institute, Sichuan University, Chengdu 610065, China xiahs@scu.edu.cn
¹¹⁰ † Electronic Supplementary Information (ESI) available: Additional details on synthesis and characterizations are given in supporting information.

- 1 (a) A. S. Hoffman, *Adv. Drug Deliv. Rev.* 2002, **54**, 3-12. (b) L. Yu and J. Ding, *Chem. Soc. Rev.* 2008, **37**, 1473-1481.
 2 (a) R. J. Russell, M. V. Pishko, C. C. Gefrides, M. J. McShane and G. L.Cote, *Anal. Chem.* 1999, **71**, 3126-3132. (b) S. Brahim, D.

- Narinesingh and A. Guiseppi-Elie, *Biosens. Bioelectron.* 2002, **17**, 53-59.
- 3 (a) M. Otake, Y. Kagami, M. Inaba and H. Inoue, *Rob. Auton. Syst.* 2002, **40**, 185-191. (b) G. H. Kwon, Y. Y. Choi, J. Y. Park, D. H. Woo, K. B. Lee, J. H. Kim and S. H. Lee, *Lab Chip* 2010, **10**, 1604-1610.
- 4 J. L. Drury and D. J. Mooney, *Biomaterials* 2003, **24**, 4337-4351.
- 5 (a) A. Phadke, C. Zhang, B. Arman, C-C. Hsu, R. A. Mashelkar, A. K. Lele, M. J. Tauber, G. Arya and S. Varghese, *PNAS* 2012, **109**, 4383-4388. (b) H. Zhang, H. Xia and Y. Zhao, *ACS Macro Lett.* 2012, **1**, 1233-1236. (c) J. Cui and A. Campo, *Chem. Commun.* 2012, **48**, 9302-9304. (d) J. Liu, G. Song, C. He and H. Wang, *Macromol. Rapid Commun.* 2013, **34**, 1002-1007. (e) K. Haraguchi, K. Uyama, and H. Tanimoto, *Macromol. Rapid Commun.* 2011, **32**, 1253-1258.
- 10 6 (a) A. B. South and L. A. Lyon, *Angew. Chem. Int. Ed.* 2010, **49**, 767-771. (b) Q. Wang, J. L. Mynar, M. Yoshida, E. Lee, M. Lee, K. Okura, K. Kinbara and T. Aida, *Nature* 2010, **463**, 339-343. (c) J.-Y. Sun, X. Zhao, W. R. K. Illeperuma, O. Chaudhuri, K. H. Oh, D. J. Mooney, J. J. Vlassak and Z. Suo, *Nature* 2012, **489**, 133-136. (d) T. Sun, T. Kurokawa, S. Kuroda, A. Ihsan, T. Akasaki, K. Sato, M. Haque, T. Nakajima and J. Gong, *Nature Materials* 2013, **12**, 932-937.
- 7 (a) F. Liu, F. Li, G. Deng, Y. Chen, B. Zhang, J. Zhang and C-Y. Liu, *Macromolecules* 2012, **45**, 1636-1645. (b) G. Deng, C. Tang, F. Li, H. Jiang and Y. Chen, *Macromolecules* 2010, **43**, 1191-1194. (c) Y. Zhang, L. Tao, S. Li and Y. Wei, *Biomacromolecules* 2011, **12**, 2894-2901. (d) L. He, D. E. Fullenkamp, J. G. Rivera and P. B. Messersmith, *Chem. Commun.* 2011, **47**, 7497-7499. (e) M. Nakahata, Y. Takashima, H. Yamaguchi and A. Harada, *Nat. Commun.* 2011, **2**, 511. (f) Y. Zhang, B. Yang, X. Zhang, L. Xu, L. Tao, S. Li and Y. Wei, *Chem. Commun.* 2012, **48**, 9305-9307.
- 8 Y. Xu, Q. Wu, Y. Sun, H. Bai and G. Shi, *ACS Nano* 2010, **4**, 7358-7362.
- 9 Z. Wei, J. He, T. Liang, H. Oh, J. Athas, Z. Tong, C. Wang and Z. Nie, *Polym. Chem.* 2013, **4**, 4601-4605.
- 10 (a) C. T. S. W. P. Foo, J. S. Lee, W. Mulyasasmita, A. Parisi-amon and S. C. Heilshorn, *PNAS* 2009, **106**, 22067-22072. (b) E. A. Appel, F. Biedermann, U. Rauwald, S. T. Jones, J. M. Zayed and O. A. Scherman, *J. Am. Chem. Soc.* 2010, **132**, 14251-14260. (c) P. J. Skrzyszewska, J. Sprakel, F. A. Wolf, R. Fokkink, M. A. C. Stuart and J. Gucht, *Macromolecules* 2010, **43**, 3542-3548.
- 11 (a) N. Holten-Andersen, M. J. Harrington, H. Birkedal, B. P. Lee, P. B. Messersmith, K. Y. C. Lee and J. H. Waite, *PNAS* 2011, **108**, 2651-2655. (b) Z. Shafiq, J. Cui, L. Pastor-Perez, V. San Miguel, R. A. Gropeanu, C. Serrano and A. Campo, *Angew. Chem. Int. Ed.* 2012, **51**, 4332-4335.
- 12 (a) P. Froimowicz, D. Klinger and K. Landfester, *Chem. Eur. J.* 2011, **17**, 12465-12475. (b) S. B. Quint and C. Pacholski, *Soft Matter* 2011, **7**, 3735-3738.
- 13 (a) D. Tuncaboylu, M. Sari, W. Oppermann and O. Okay, *Macromolecules* 2011, **44**, 4997-5005. (b) D. C. Tuncaboylu, A. Argun, M. P. Algi and O. Okay, *Polymer* 2013, **54**, 6381-6388.
- 14 (a) Y. Osada and A. Matsuda, *Nature* 1995, **376**, 219. (b) J. Hao and R. A. Weiss, *ACS Macro Lett.* 2013, **2**, 86-89. (c) U. Nöchel, C. S. Reddy, N. K. Uttamchand, K. Krat, M. Behla and A. Lendlein, *Eur. Polym. J.* 2013, **49**, 2457-2466. (d) K. Inomata, T. Terahama, R. Sekoguchi, T. Ito, H. Sugimoto and E. Nakanishi, *Polymer* 2012, **53**, 3281-3286. (e) O. Peters and H. Ritter, *Angew. Chem. Int. Ed.* 2013, **52**, 8961-8963. (f) C. Bilici and O. Okay, *Macromolecules* 2013, **46**, 3125-3131.
- 15 See, for example: (a) Y. Amamoto, J. Kamada, H. Otsuka, A. Takahara and K. Matyjaszewski, *Angew. Chem. Int. Ed.* 2011, **50**, 1660-1663. (b) G. Li, G. Fei, H. Xia, J. Han and Y. Zhao, *J. Mater. Chem.* 2012, **22**, 7692-7696. (c) C. C. Corten and M. W. Urban, *Adv. Mater.* 2009, **21**, 5011-5015. (d) M. Y. Razaq, M. Behl and A. Lendlein, *Adv. Funct. Mater.* 2012, **22**, 184-191. (e) M. V. Biyani, E. J. Foster and C. Weder, *ACS Macro Lett.* 2013, **2**, 236-240. (f) B. Michal, C. A. Jaye, E. J. Spencer and S. J. Rowan, *ACS Macro Lett.* 2013, **2**, 236-240.
- 16 F. Dutertre, P. Pennarun, O. Colombani and E. Nicol, *Eur. Polym. J.* 2011, **47**, 343-351.

Graphic for Table of Contents

5



AuNP-containing hard hydrogel based on coexisted chemical and physical crosslinking can have damage healed by laser exposure as a result of the melting-crystallization phase transition of the dangling hydrophobic side chains.